Loss of acid sphingomyelinase ameliorates disease progression in a vertebrate model of Glucocerebrosidase deficiency

Marcus Keatinge[1,2,3*], Matthew E. Gegg[4*], Lisa Watson[1,2], Heather Mortiboys[2], Hai Bui[5], Astrid van Rens[6], Dirk J.Lefeber[6,7], Ryan B. MacDonald[1], Anthony H.V. Schapira[4], Oliver Bandmann[1,2]

*Both authors contributed equally to the manuscript.

[1]Bateson Centre, Firth Court, University of Sheffield, Western Bank Sheffield S10 2TN, UK and [2]Sheffield Institute for Translational Neuroscience (SITraN), University of Sheffield, 385a Glossop Road, Sheffield S10 2HQ, UK; [3]Centre for Discovery Brain Sciences, Chancellor's Building, Edinburgh EH16 4TJ, UK; [4]Department of Clinical and Movement Neurosciences, UCL Queen Square Institute of Neurology, London NW3 2PF, UK; [5]Eli Lilly and Company, Drop Code 1940,Indianapolis, IN 46285 USA; [6]Department of Laboratory Medicine, Translational Metabolic Laboratory, Radboud University Medical Center, Nijmegen, The Netherlands. [7]Department of Neurology, Donders Institute for Brain, Cognition and Behaviour, Radboud University Medical Center, Nijmegen, The Netherlands.

Address corresponding author: Prof Oliver Bandmann MD PhD, Sheffield Institute for Translational Neuroscience, Sheffield Institute for Translational Neuroscience (SITraN), 385a Glossop Road, Sheffield S10 2HQ, UK. Tel: x44-114-2222261; email: o.bandmann@sheffield.ac.uk.

Abstract

Biallelic *glucocerebrosidase (GBA)* mutations cause the lysosomal storage disorder Gaucher disease (GD), while heterozygous *GBA* variants are the strongest and most common genetic risk factor for Parkinson disease (PD). An excessive burden of other lysosomal storage disorder gene variants, in particular for *SMPD1* (encoding for acid sphingomyelinase (ASM)) has also been reported in PD. However, it is unclear whether *GBA* and *SMPD1* interact genetically. Zebrafish are an ideal vertebrate system to test for such interactions. We previously characterised a *gba1*$^{-/-}$ mutant zebrafish line which displayed key hallmarks of human GD. In this work, we describe the biological interaction of combined glucocerebrosidase (GCase) and ASM deficiency in *gba1*$^{-/-}$;*smpd1*$^{-/-}$ double mutant zebrafish. We observed a marked increase of glucosylceramide, ceramide and other key sphingolipids or their metabolites in *gba1*$^{-/-}$;*smpd1*$^{-/-}$ compared to *gba1*$^{-/-}$ or *smpd1*$^{-/-}$ zebrafish. Unexpectedly, we observed a marked ameliorating effect of ASM inactivation on behaviour and disease duration in *gba1*$^{-/-}$, resulting in a rescue of the characteristic motor phenotype and improved survival in *gba1*$^{-/-}$*;smpd1*$^{-/-}$. We identified complete rescue of mitochondrial respiratory chain function with normalisation of lipid peroxidation as the underlying mechanism for the observed rescue effect in *gba1*$^{-/-}$;*smpd1*$^{-/-}$. Combined ASM knockdown and GCase inhibition in human neuroblastoma SH-SY5Y cells unexpectedly lead to a decrease in monomeric α-synuclein, a key pathogenic protein in PD, which was independent of changes in macroautophagy flux. Our work highlights the importance of investigating the downstream functional consequences of gene-gene interactions in complex interacting pathways to determine any composite risk.

Keywords:

Parkinson's disease, glucocerebrosidase 1, acid sphingomyelinase, zebrafish, gene-gene interaction.

Significance statement:

The additive effect of genetic risk variants on disease incidence is a popular but frequently unproven hypothesis. Variants in the lysosomal disease genes *glucocerebrosidase1* (*GBA1*) and *sphingomyelinase* (*SMPD1*) are risk factors for Parkinson's disease (PD). Zebrafish are ideally suited to study gene-gene interaction. We investigated a genetic interaction between *gba1*$^{-/-}$ and *smpd1*$^{-/-}$ in *gba1*$^{-/-}$;*smpd1*$^{-/-}$ double-mutant zebrafish and observed an unexpected ameliorating effect of sphingomyelinase deficiency on the *gba1*$^{-/-}$ related phenotype with prolonged survival and normalisation of motor behaviour due to rescue of mitochondrial function. Complementing experiments in SH-SY5Y neuroblastoma cells revealed an unexpected lowering of α-synuclein in the presence of combined glucocerebrosidase and sphingomyelinase inhibition. Our study highlights the importance of functional validation for any putative gene-gene interactions.

Introduction

Monogenically inherited forms of Parkinson's disease (PD) due to mutations in Mendelian PARK genes such as *SNCA*, *LRRK2* or *parkin* can only be detected in 5-10% of PD patients in most populations (1). Hypothesis-driven research combined with genome-wide association studies (GWAS) have identified > 30 putative or definitive PD risk genes but the effect of each individual risk gene is typically small (2). A popular but largely unproven hypothesis is an additive effect of risk haplotypes, based on the assumption that the risk of PD correlates with the number of risk variants present in an individual.

Biallelic mutations in the *glucocerebrosidase 1* (*GBA1)* gene lead to the lysosomal storage disorder Gaucher's disease (GD). Genetic inactivation of *GBA1* results in decreased activity of the lysosomal enzyme glucocerebrosidase (GCase) which hydrolyses glucosylceramide to ceramide and glucose. The key pathological feature of GD is the accumulation of lipid laden macrophages called "Gaucher cells", resulting in splenomegaly, hepatomegaly and dysfunction of other organs including the brain (3, 4). Three subtypes of GD with markedly different age at onset and disease severity are recognized but the factors influencing the specific disease phenotype in individual GD patients are largely unknown (5). Heterozygous *GBA1* mutations are the most common and strongest genetic risk factor for the common neurodegenerative disorder Parkinson's disease (PD) with a prevalence of ~ 5-20%, depending on the population investigated (6-8). Heterozygote *GBA1* mutation carriers have a 10%-30% risk of developing PD by age 80 up to a 20-fold increase compared to non-carriers (9, 10). Severe *GBA1* mutations confer a considerably higher risk of PD than mild mutations (11). However, no additional factors other than age or the severity of the *GBA1* mutation have been identified which would explain the highly variable penetrance of PD in *GBA1* mutations carriers. Of note, sequence variants in other lysosomal disease genes (LSD) were subsequently identified as additional and separate risk factors for

PD (12). There is particularly strong evidence for an association with variants in the *SMPD1* gene (encoding for acid sphingomyelinase (ASM)), the causative gene of Niemann-Pick disease A/B (13).

Zebrafish (*Danio rerio*) are an ideally suited vertebrate model to study gene-gene interactions due to their short generation time, high fecundity and ease of housing. Gene editing tools such as transcription activator-like effector nucleases (TALENs) or clustered regular interspersed short palindromic repeat (CRISPR) systems are widely used in zebrafish research (14). We had previously characterised a *gba1* mutant zebrafish line *(gba1*$^{-/-}$*)* (15). *gba1*$^{-/-}$ zebrafish faithfully modelled key features of GD including Gaucher cell accumulation, marked microglial infiltration and neurodegeneration. *gba1*$^{-/-}$ larvae develop normally despite crucial consequences of GCase deficiency such as early microglial activation and GCase substrate accumulation already being present at 5 days post fertilization (dpf). From 10-12 weeks onwards, *gba1*$^{-/-}$ juvenile zebrafish rapidly deteriorate and die or must be culled for animal welfare reasons at 12-14 weeks.

As both GCase and ASM are lysosomal hydrolases linked to sporadic PD, we hypothesised that ASM deficiency could accelerate disease progression and enhance the phenotype in GCase deficient *gba1*$^{-/-}$ zebrafish. Unexpectedly, we observed a rescue effect of ASM deficiency with prolonged survival due to marked improvement of mitochondrial function and reduced oxidative stress in *gba1*$^{-/-}$*;smpd1*$^{-/-}$ zebrafish. Complementary work in human neuroblastoma SH-SY5Y cells demonstrated that dual ASM and GCase deficiency also results in a significant decrease in α-synuclein levels (when compared to cells with just GCase deficiency) which is not due to changes to macroautophagy flux.

Results

smpd1$^{-/-}$ zebrafish display abolished acid sphingomyelinase activity and marked sphingolipid accumulation

We identified a single *smpd1* orthologue in zebrafish (ENSDARG00000076121) with 59% shared identity to the human *SMPD1* gene at both the DNA and the protein level. CRISPR/Cas9 technology was used to generate a *smpd1* stable mutant line *(smpd1*$^{-/-}$*).* The selected mutant allele contained a 5bp deletion and 136bp insertion within exon 3, resulting in a frame-shift and the generation of a premature stop codon (Fig. 1*A* and *SI Appendix* Fig. S1). Enzymatic activity of ASM in *smpd1*$^{-/-}$ at 5 dpf was reduced by 93% (4.3 nmol/18 h/mg protein, n=6 vs. 64 nmol/18 h/mg protein, n= 7, p=0.006, Welch's two--tailed-t-test, Fig. 1*B*).

The large reduction in ASM enzymatic activity resulted in a significant increase of key glycolipid substrates in the *smpd1*$^{-/-}$ larvae already at 5 dpf (Fig. 1*C*). This included sphingomyelin (102% increase, p=0.0002), di-hydrosphingomyelin (105% increase, p=0.004), ceramide (27% increase, p=0.0067), lactosylceramide (50% increase, p=0.0191), sphinganine (114% increase, p=0.0007) and sphinganine-1-phosphate (80% increase, p=0.0093).

Combined ASM and GCase deficiency synergistically increases sphingolipid metabolites

We had previously reported marked sphingolipid accumulation in *gba1*$^{-/-}$ zebrafish (15). We hypothesised that combined (enzymatic) GCase and ASM deficiency would synergistically increase distinct sphingolipid subtypes. Using mass spectrometry, a comprehensive panel of glycolipid substrates was analysed in the brains of *gba*$^{-/-}$ and *smpd1*$^{-/-}$ (single mutant) as well as in *gba*$^{-/-}$*;smpd1*$^{-/-}$ (double mutant) zebrafish and WT controls at 12 weeks of age.

Glucosylceramide levels (the direct substrate of GCase) were not significantly changed in *smpd1*$^{-/-}$ brains compared to WT, but were increased by 31517% above WT levels in *gba1*$^{-/-}$ brains ($p<0.0001$, Fig. 2A) with a further marked synergistic increase in glucosylceramide levels by 16609% in the *gba*$^{-/-}$*;smpd1*$^{-/-}$ double mutants with glucosylceramide levels reaching an increase of 48126% compared to WT ($p<0.0001$, Fig. 2*A*).

Lactosylceramide levels demonstrated a similar trend across the four genotypes. *smpd1*$^{-/-}$ brains did not have a significant increase in lactosylceramide levels compared to WT, but *gba1*$^{-/-}$ showed a marked increase of 4028% compared to WT ($p<0.0001$, Fig. 2*B*) and there was then a further synergistic increase in *gba*$^{-/-}$*;smpd1*$^{-/-}$ double mutants to 4724% above WT levels ($p<0.0001$, Fig. 2*B*). This 696% increase in lactosylceramide levels between *gba*$^{-/-}$ and *gba*$^{-/-}$*;smpd1*$^{-/-}$ again demonstrated synergy between the two different genotypes ($p=0.0191$).

Ceramide levels were raised by 106% in *smpd1*$^{-/-}$ and 88% in *gba1*$^{-/-}$ compared to WT ($p<0.0001$ for both, Fig. 2*C*), with *gba*$^{-/-}$*;smpd1*$^{-/-}$ showing an additive 200% ceramide increase compared to WT ($p<0.0001$ compared to *gba1*$^{-/-}$, *smpd1*$^{-/-}$ and WT, Fig. 2*C*). Sphinganine levels were raised by 95% in *smpd1*$^{-/-}$ ($p<0.0001$ Fig. 2*D*) and by 46% in *gba1*$^{-/-}$ ($p=0.0383$, Fig. 2*D*) and an increase by 225% in *gba*$^{-/-}$*;smpd1*$^{-/-}$ compared to WT ($p<0.0001$ compared to *gba1*$^{-/-}$, *smpd1*$^{-/-}$ and WT).

Similarly but in a less pronounced manner, sphingosine levels were increased in *smpd1*$^{-/-}$ by 60% compared to WT (p<0.0001, Fig. 2*E*) but only increased by 35% in *gba1*$^{-/-}$ (p=0.0025, Fig. 2*E*). Sphingosine levels were increased to 84% in *gba*$^{-/-}$*;smpd1*$^{-/-}$ compared to WT (p<0.0001, Fig. 2E), reflecting an significant increase compared to *gba1*$^{-/-}$ (p<0.0001, Fig. 2*E*) but not compared to *smpd1*$^{-/-}$ (p>0.05, Fig. 2*E*). In contrast, Sphingomyelin, the direct substrate of acid sphingomyelinase had a marked accumulation of 288% in *smpd1*$^{-/-}$ compared to WT levels (p<0.0001, Fig. 2*F*), but was unchanged in *gba1*$^{-/-}$. Unexpectedly, there was no synergistic effect in sphingomyelin levels in the double mutants, which demonstrated a comparable increase to that seen in *smpd1*$^{-/-}$ compared to WT of 309% (p<0.0001, Fig. 2*F*).

Chitotriosidase and β-Hexosaminidase are markedly increased in the serum of GD patients and used as biomarkers to monitor disease activity (3). We previously observed a marked increase in chitotriosidase and β-hexosaminidase activity in *gba1*$^{-/-}$ zebrafish brain tissue at 12 weeks (15). As key GCase substrates were synergistically increased in *gba*$^{-/-}$*;smpd1*$^{-/-}$ double mutant zebrafish, we investigated whether combined GCase and ASM inactivation may also result in a further increase chitotriosidase and β-hexosaminidase activity (*SI Appendix*, Fig 2). As expected, β-hexosaminidase activity was similar in *smpd1*$^{-/-}$ and WT, but markedly elevated in *gba1*$^{-/-}$ by 85% (2284±200 nmol/hr/mg protein, p<0.0001, n= 5, *SI Appendix,* Fig. 2A) compared to WT (1234±47.3nmol/hr/mg protein). Unexpectedly, double mutants displayed a similar increase in activity to *gba1*$^{-/-}$ by 70% (2131±272.2nmol/hr/mg protein, p<0.0001, n=5, *SI Appendix,* Fig. 2A) compared to WT. Chitotriosidase activity was again similar in *smpd1*$^{-/-}$ compared to WT, but markedly increased in *gba1*$^{-/-}$ by 389% (31.8±11.95 nm/hr/mg protein, p=0.0002, n=5, *SI Appendix,* Fig. 2B) compared to WT levels (6.5±4.0 nm/hr/mh protein n=5). Brains from *gba*$^{-/-}$*;smpd1*$^{-/-}$ double mutant zebrafish showed a large 230% increase in chitotriosidase activity (21.5±5.1nm/hr/mg protein, p=0.0177, n=5 *SI Appendix,* Fig. 2B) compared to WT.

Although this increase was not as large as that seen in *gba1*$^{-/-}$ (230% increase compared to 389% increase), the differences in activities between *gba1*$^{-/-}$ and double mutants was not significant. β--galactosidase activity was used a control enzyme and as expected, all genotypes showed comparable activities of approximately 50nm/hr/mg protein, (n=5 for all genotypes, *SI Appendix,* Fig. 2*C*).

Acid sphingomyelinase deficiency prolongs survival of *gba*$^{-/-}$ due to rescue of mitochondrial function and reduction of oxidative stress

The marked synergistic effect of combined deficiency of GCase and acid sphingomyelinase activity on key sphingolipids in the *gba*$^{-/-}$*;smpd1*$^{-/-}$ double mutant zebrafish suggested a possible effect of ASM activity on clinically relevant aspects of our *gba1*$^{-/-}$ zebrafish, in particular behaviour and survival. End stage *gba1*$^{-/-}$ mutants exhibit very robust behavioural phenotypes with barrel rolling like behaviour (15). Unexpectedly, genetic inactivation of ASM led to a complete rescue of this behaviour in the *gba*$^{-/-}$*;smpd1*$^{-/-}$ double mutant zebrafish (*SI Appendix,* Video S1 (WT), S2 (*smpd1*$^{-/-}$), S3 (*gba1*$^{-/-}$) and S4 (*gba*$^{-/-}$*;smpd1*$^{-/-}$)). We also observed a marked increase in lifespan by 23 days (22%) in *gba1*$^{-/-}$;*smpd1*$^{-/-}$ double mutant zebrafish compared to *gba1*$^{-/-}$ (median survival of 102 dpf in *gba1*$^{-/-}$ and 125dpf in *gba1*$^{-/-}$;*smpd1*$^{-/-}$, p=0.0055, Fig. 3*A*).

Mitochondrial function is markedly impaired in GCase deficiency and other lysosomal storage disorders (16, 17). We had previously observed a marked reduction of mitochondrial respiratory chain Complex IV activity and, to a lesser extent, also of Complex III in *gba1*$^{-/-}$ (15). We hypothesised that the observed partial rescue effect of acid sphingomyelinase deficiency on behaviour and survival of the *gba*$^{-/-}$ zebrafish may be due to a rescue of the impaired mitochondrial respiratory chain function. As predicted, mitochondrial dysfunction in both *gba*$^{-/-}$ and *smpd1*$^{-/-}$ zebrafish improved considerably in *gba1*$^{-/-}$;*smpd1*$^{-/-}$. Complex I activity was reduced by 65% in *smpd1*$^{-/-}$

compared to WT levels (p=0.0198, Fig 3*B*) but restored to 92% of WT levels in *gba1*$^{-/-}$;*smpd1*$^{-/-}$ (p=0.0445, Fig 3*B*). Complex II was not significantly altered in any of the genotypes (Fig. 3*C*). Complex III activity in *gba1*$^{-/-}$ was reduced by 45% compared to WT levels (p=0.0091, Fig. 3*D*) as previously observed (15). In contrast, Complex III activity in the *gba1*$^{-/-}$;*smpd1*$^{-/-}$ double mutant zebrafish was reduced by only 9% compared to WT levels and thus considerably less pronounced than the reduction observed in the *gba1*$^{-/-}$, suggesting a rescue effect in *gba1*$^{-/-}$;*smpd1*$^{-/-}$. However, this 36% increase in complex III activity in *gba1*$^{-/-}$;*smpd1*$^{-/-}$ compared to *gba1*$^{-/-}$ did not reach statistical significance. Complex IV activity was unchanged in *smpd1*$^{-/-}$ compared to WT, but reduced by 40% in *gba1*$^{-/-}$ compared to WT as previously reported (p=0.0491, Fig. 3*E*). Remarkably, there was a marked improvement of complex IV activity in *gba1*$^{-/-}$;*smpd1*$^{-/-}$ with an increase in activity of 69% compared to *gba1*$^{-/-}$ (p= 0.0005, Fig. 3*E*).

Malfunction of the mitochondrial respiratory chain can result in oxidative stress and subsequent lipid peroxidation. We therefore investigated next whether the observed rescue in mitochondrial function results in reduced oxidative stress-related damage. Lipid peroxidation was increased in *gba1*$^{-/-}$ brains by 63% above WT levels (p= 0.0214, Fig. 3*F*). As predicted, lipid peroxidation levels were reduced by 70% in *gba1*$^{-/-}$;*smpd1*$^{-/-}$ double mutants compared to *gba1*$^{-/-}$ and thus effectively normalized (p=0.0094, Fig. 3*F*).

Dual GCase and ASM inhibition leads to a decrease in α-synuclein levels

Given the effect of (isolated) GCase or ASM deficiency on α-synuclein in PD (13, 18), we also wanted to investigate the effect of combined GCase and ASM deficiency on α-synuclein homeostasis. The zebrafish genome does not contain α-synuclein. We therefore investigated the combined effect of ASM and GCase deficiency on α-synuclein homeostasis in a previously established human dopaminergic SH-SY5Y neuroblastoma cell line (19). A siRNA-approach was applied to inactivate

SMPD1/ASM, GCase was inhibited with conduritol B-epoxide (CBE) for 10 days (19). *SMPD1* mRNA levels in the absence or presence of CBE were significantly decreased relative to scrambled (scram) control treated cells (65±19% and 64±15% reduction, respectively; *p* =0.0003 and 0.0007, Fig 4A]. Treatment with CBE alone or in the presence of *SMPD1* siRNA significantly decreased GCase activity [79% and 76% reduction, respectively; *P*< 0.01)] relative to scram treated cells (19). Notably GCase activity was significantly increased in *SMPD1* knock down cells, compared to scram (15% increase; *P* < 0.05, Fig 4B). Unexpectedly, the levels of α-synuclein were significantly decreased (rather than increased as predicted) in *SMPD1*-KD + CBE-treated cells (42% reduction relative to scram treated cells; p=0.0139, Fig. 4*C* and *D*), when compared to CBE-treated cells. The decrease in intracellular α-synuclein levels in *SMPD1-KD*+CBE was not due to increased release of α-synuclein in to the media (Fig. 4E) or becoming insoluble (data not shown). Inhibition of ASM is known to promote autophagy (20). We (MG, AS) and others had previously observed impaired autophagy/mitophagy in GCase deficiency (19, 21, 22). We therefore assessed next whether the observed reduction in α-synuclein levels may be due to enhanced autophagy in tissue which is both GCase and ASM deficient. We measured macroautophagy flux by measuring the levels of LC3-II by western blot, a marker for autophagosome number. Under basal conditions, LC3-II levels were similar in all groups. As expected treatment with bafilomycin A1, which prevents the fusion of lysosomes with autophagosomes, caused an accumulation of autophagosomes, and was similar in all groups (Fig. 4*F-G*). These data suggest that there is neither an impairment nor increase in macroautophagy flux under any conditions.

The detection of acidic vesicles (e.g. endosome and lysosomes) in live cells with the fluorescent probe LYSO-ID indicated a significant increase in the number of acidic vesicles in both *SMPD1* KD (31169±5012 fluorescent units/mg; p=0.0275, *SI Appendix*, Fig. S3*A*) and *SMPD1* KD + CBE cells (29600±7758 fluorescent units/mg;

p=0.0452, *SI Appendix*, Fig. S3*A*), relative to scram cells (15180±2853 fluorescent units/mg; *SI Appendix*, Fig. S3*A*). Of note, there was only a trend towards an increase in the number of acidic vesicles in CBE treated cells but no additive effect in cells with combined acid sphingomyelinase and GCase inhibition. The protein levels of the endolysosomal protein LAMP1 were not significantly changed, although there was a trend towards an increase of LAMP1 protein levels in *SMPD1* KD cells (*SI Appendix*, Fig. S3*B*). Chaperone mediated autophagy (CMA) degrades substrates containing the pentapeptide sequence KFERQ. The chaperone hsc70 binds proteins with this motif and moves to the lysosome, whereupon it passes the substrate onto LAMP2A, which translocates the protein for degradation in to the lumen of lysosomes (23). LAMP2A protein levels were significantly decreased in *SMPD1* KD cells (47% reduction; p=0.0257, *SI Appendix*, Fig. S3*C*+*D*) relative to scram-treated cells. LAMP2A protein levels in *SMPD1* KD + CBE cells were decreased by 35%, although not significantly (*SI Appendix*, Fig. S3C+D). The protein levels of hsc70 were not significantly different between the groups (scram, 0.94 ± 0.08 hsc70/GAPDH; scram + CBE, 0.95 ± 0.13; *SMPD1*-KD, 0.81 ± 0.13; *SMPD1*-KD + CBE, 0.94 ± 0.11). Increased cholesterol levels in lysosomal membranes have been reported to promote the degradation of LAMP2A. However, no significant changes in either total cellular cholesterol levels, or its localisation were detected in *SMPD1*-KD cells, relative to the other groups (*SI Appendix*, Fig. S3*E*+*F*).

Discussion

Both *GBA1* and *SMPD1* variants are firmly established inherited risk factors for PD. Additional lysosomal storage disease (LSD) genes such as *CTSD*, *SLC17A5* and *ASAH1* have also been implicated (12, 24). Biochemically, GCase and acid sphingomyelinase both play a key role in sphingolipid metabolism (25). We therefore hypothesized that ASM deficiency would further enhance the phenotype and accelerate disease progression in GCase-deficient zebrafish. However, unexpectedly, we observed a rescue of the "barrel-rolling" phenotype and a marked prolongation of life expectancy despite clear evidence of an additive effect of the key sphingolipids and their metabolites. The remarkable rescue effect of mitochondrial function in *gba1*$^{-/-}$;*smpd1*$^{-/-}$ on behaviour and survival suggests a central role of mitochondrial dysfunction in GCase deficiency. The observation of normalised mitochondrial respiratory chain function and amelioration of lipid peroxidation in *gba*$^{-/-}$;*smpd1*$^{-/-}$ would be comparable with the assumption of enhanced mitophagy which would be in keeping with the well-established autophagy-enhancing effect of acid sphingomyelinase inhibition (20, 26, 27). Partial ASM inhibition restored autophagic dysfunction in AD patient-derived neurons as well as ameliorating the autophagic defect in in AD mice, resulting in a reduction of amyloid-beta deposition and improved memory impairment (28). However, in our human dopaminergic cell culture models, macroautophagy flux appeared unaffected in either ASM deficiency alone, or in cells with both decreased ASM and GCase. It should be noted that we had previously observed > 95% GCase inhibition after treatment with 10 uM CBE (19), whereas GCase activity was reduced to ~ 80% only in the presence of the transfection reagent required for the knockdown of ASM in this study. This likely explains why the trend for increased α-synuclein levels in the CBE-only treatment arm was not statistically significant but is still comparable to previous results from CBE-mediated GCase inhibition in SH-SY5Y cells (19) and mouse brain (29). The remarkable decrease in soluble monomeric α-synuclein in cells with combined ASM and GCase deficiency may reflect a link between tightly controlled

sphingolipid metabolism and α-synuclein homeostasis. However, the zebrafish genome does not contain an orthologue of α-synuclein. Thus, the observed partial rescue effect of ASM deficiency in our GCase deficient zebrafish model cannot be due to modulation of α-synuclein levels in *gba*$^{-/-}$;*smpd1*$^{-/-}$. Given both enzymes are involved in sphingolipid metabolism, it is probable that changes in the glycosphingolipid profile of the cell contribute to the changes observed. Previous reports have also demonstrated that modulation of the glycosphingolipid profile in GCase deficient cells, other than restoration of GCase activity, can improve α-synuclein homeostasis (30, 31).

Although unexpected, we are not the first to report a rescue effect of double knockout of lysosomal hydrolases or their paralogues. *GBA2* inactivation had a marked rescue effect on the phenotype typically observed in conditional *GBA1* knockout mouse models, whilst simultaneous knock out of galactosylceramidase and beta galactosidase dramatically extended lifespan of galactosylceramidase knockout mice (32, 33). Zebrafish are ideally suited to study gene-gene interactions in a vertebrate model system of human disease (34-37). Future studies are needed to determine the functional interaction of other PD risk genes, especially those acting in shared pathways such as LSD genes.

Materials and Methods

Zebrafish husbandry. All larval and adult zebrafish were housed at the University of Sheffield; experimental procedures being in accordance UK Home Office Animals (Scientific Procedures) Act 1986 (Project license PPL 70/8437, held by Dr Oliver Bandmann). Adult zebrafish were housed at a density of 20 per tank, on a cycle of 14 h of light, 10 h of dark. Adults and embryos were kept at constant temperature of 28°C.

Mutant line generation and line maintenance. *The gba1*$^{-/-}$ mutant lines was generated using TALEN technology(15). The *smpd1*$^{-/-}$ mutant line was generated by the Crispr/Cas9 method as previously described (38). The following ultramer template was used: 5'-AAAGCACCGACTCGGTGCCACTTTTTCAAGTTGATAACGGACTAGCCTTATTTTAACTTGCTATTTCTAGCTCTAAAACGGATTGAGGCTTGTGTCTCcCTATAGTGAGTCGTATTACGC). The *smpd1*$^{-/-}$ line was genotyped using primers F 5'-AGCCGTGGTGGTTTCTACAG and R 5'-CCTTCTCTCCCTTGTTCTCG. The *smpd1*$^{-/-}$ line was crossed to *gba1*$^{+/-}$ to generate double heterozygous individuals. These were subsequently in-crossed to generate double mutants. At each in-cross larvae were genotyped at 3dpf by larval tail biopsy as previously described (39). Each genotyped was raised in genotype-specific tanks at a density of 10-15 fish per tank. All individuals were re-genotyped at 10 weeks post-fertilisation. *smpd1*$^{+/-}$ were crossed with *gba1*$^{+/-}$ to generate *gba1*$^{+/-}$*;smpd1*$^{+/-}$*.* These were subsequently in-crossed to generate double mutants, single mutants and WT controls.

Biochemical activity assays and mass spectrometry. Sphingomyelinase activity was determined using homogenates prepared as follows. Tubes containing twenty embryos (5 dpf) were sonicated in 500 µl MilliQ and centrifuged (11000 rpm). ASM activities were measured using 20 µL supernatant and incubated with substrate HMU-PC (6-hexadecanoylamino-4-methylumbelliferyl-phosphorylcholine 0.66 mM, 20 µL,

Moscerdam Substrates, NL) at pH 5.2 and 37 °C during 2 hours. Fluorescence intensity was measured at 415 (ex) and 460 (em) nm using a plate reader (LS55, Perkin Elmer). Lysosomal and mitochondrial enzyme assays as well as mass spectrometry were undertaken as previously described (15).

Lipid peroxidation assay. Mitochondria were isolated from the bodies of 3 month old zebrafish. Bodies were homogenised in ice cold mitochondrial isolation buffer. The Abcam lipid peroxidation kit (ab118970) fluorimetric assay was used to measure lipid peroxidation according to manufacturer's instructions. Results were normalised to WT.

Cell culture experiments. SH-SY5Y cells were cultured in DMEM:F12 (1:1) supplemented with 10% foetal calf serum, 1 mM sodium pyruvate, non-essential amino acids and antibiotics. Cells were passaged and transfected every 72 hours with 12.5 nM SMPD1 ON-TARGETplus SMARTpool siRNA (Dharmacon) using HiPerfect transfection reagent (Qiagen) in the absence or presence of 10 μM CBE up to 10 days in culture. Antibodies used were: rabbit LAMP2A antibody (abcam ab125068, 1:1000), mouse α-synuclein antibody (abcam ab27766, 1:1000), mouse LAMP1 antibody (Novus Biologicals NPB2-25155, 1:8000). Human α-synuclein in cell culture media was detected using LEGEND MAX ELISA kit (BioLegend). Total cholesterol levels were measured using the Amplex Red Cholesterol Assay Kit (Invitrogen), while the localisation of cholesterol was detected using Filipin III as per manufacturer's instructions (abcam ab 133116). Fillipin staining was assessed using a Nikon Eclipse Ti_E inverted microscope (excitation 340 nm and emmission 460 nm; 40X magnification). Images were acquired using a Hamamatsu Orca-Flash camera and NIS Elements AR software.

Statistical analysis. Graphpad prism V.6 software (Graphpad) was used for statistical analysis and all errors bars shown denote the mean ± SD of the mean. All experiments

were performed in biological triplicate unless otherwise stated. All data were analysed with either T test, two-way ANOVA. Significance in all enzyme activity assays was determined by two way ANOVA with Tukey's multiple comparison test.

Acknowledgements:

This work was supported by funding from Parkinson's UK (G1404 and G1704), the Medical Research Council (MRC, MR/R011354/1 and MR/M006646/1). This research was also supported by the NIHR Sheffield Biomedical Research Centre (BRC).

References:

1. Grabowski GA (2012) Gaucher disease and other storage disorders. *Hematology Am Soc Hematol Educ Program* 2012:13-18.
2. Platt FM (2014) Sphingolipid lysosomal storage disorders. *Nature* 510(7503):68-75.
3. Baris HN, Cohen IJ, & Mistry PK (2014) Gaucher disease: the metabolic defect, pathophysiology, phenotypes and natural history. *Pediatr Endocrinol Rev* 12 Suppl 1:72-81.
4. Neumann J*, et al.* (2009) Glucocerebrosidase mutations in clinical and pathologically proven Parkinson's disease. *Brain* 132(Pt 7):1783-1794.
5. Sidransky E*, et al.* (2009) Multicenter analysis of glucocerebrosidase mutations in Parkinson's disease. *N Engl J Med* 361(17):1651-1661.
6. Siebert M, Sidransky E, & Westbroek W (2014) Glucocerebrosidase is shaking up the synucleinopathies. *Brain* 137(Pt 5):1304-1322.
7. Anheim M*, et al.* (2012) Penetrance of Parkinson disease in glucocerebrosidase gene mutation carriers. *Neurology* 78(6):417-420.
8. O'Regan G, deSouza RM, Balestrino R, & Schapira AH (2017) Glucocerebrosidase Mutations in Parkinson Disease. *J Parkinsons Dis* 7(3):411-422.
9. Gan-Or Z*, et al.* (2015) Differential effects of severe vs mild GBA mutations on Parkinson disease. *Neurology* 84(9):880-887.
10. Robak LA*, et al.* (2017) Excessive burden of lysosomal storage disorder gene variants in Parkinson's disease. *Brain* 140(12):3191-3203.
11. Alcalay RN*, et al.* (2019) SMPD1 mutations, activity, and alpha-synuclein accumulation in Parkinson's disease. *Mov Disord* 34(4):526-535.
12. Simone BW, Martinez-Galvez G, WareJoncas Z, & Ekker SC (2018) Fishing for understanding: Unlocking the zebrafish gene editor's toolbox. *Methods* 150:3-10.

13. Keatinge M*, et al.* (2015) Glucocerebrosidase 1 deficient Danio rerio mirror key pathological aspects of human Gaucher disease and provide evidence of early microglial activation preceding alpha-synuclein-independent neuronal cell death. *Hum Mol Genet* 24(23):6640-6652.

14. Gegg ME & Schapira AH (2016) Mitochondrial dysfunction associated with glucocerebrosidase deficiency. *Neurobiol Dis* 90:43-50.

15. McKenna MC, Schuck PF, & Ferreira GC (2019) Fundamentals of CNS energy metabolism and alterations in lysosomal storage diseases. *J Neurochem* 148(5):590-599.

16. Mazzulli JR*, et al.* (2011) Gaucher disease glucocerebrosidase and alpha-synuclein form a bidirectional pathogenic loop in synucleinopathies. *Cell* 146(1):37-52.

17. Magalhaes J*, et al.* (2016) Autophagic lysosome reformation dysfunction in glucocerebrosidase deficient cells: relevance to Parkinson disease. *Hum Mol Genet* 25(16):3432-3445.

18. Perrotta C*, et al.* (2015) The emerging role of acid sphingomyelinase in autophagy. *Apoptosis* 20(5):635-644.

19. Li H*, et al.* (2019) Mitochondrial dysfunction and mitophagy defect triggered by heterozygous GBA mutations. *Autophagy* 15(1):113-130.

20. Osellame LD*, et al.* (2013) Mitochondria and quality control defects in a mouse model of Gaucher disease--links to Parkinson's disease. *Cell Metab* 17(6):941-953.

21. Campbell P, Morris H, & Schapira A (2018) Chaperone-mediated autophagy as a therapeutic target for Parkinson disease. *Expert Opin Ther Targets* 22(10):823-832.

22. Gasser T (2015) Usefulness of Genetic Testing in PD and PD Trials: A Balanced Review. *J Parkinsons Dis* 5(2):209-215.

23. Chang D*, et al.* (2017) A meta-analysis of genome-wide association studies identifies 17 new Parkinson's disease risk loci. *Nat Genet* 49(10):1511-1516.

24. Ysselstein D, Shulman JM, & Krainc D (2019) Emerging links between pediatric lysosomal storage diseases and adult parkinsonism. *Mov Disord*.

25. Lin G, Wang L, Marcogliese PC, & Bellen HJ (2019) Sphingolipids in the Pathogenesis of Parkinson's Disease and Parkinsonism. *Trends Endocrinol Metab* 30(2):106-117.

26. Cervia D*, et al.* (2016) Essential role for acid sphingomyelinase-inhibited autophagy in melanoma response to cisplatin. *Oncotarget* 7(18):24995-25009.

27. Justice MJ*, et al.* (2018) Inhibition of acid sphingomyelinase disrupts LYNUS signaling and triggers autophagy. *J Lipid Res* 59(4):596-606.

28. Lee JK*, et al.* (2014) Acid sphingomyelinase modulates the autophagic process by controlling lysosomal biogenesis in Alzheimer's disease. *J Exp Med* 211(8):1551-1570.

29. Rocha EM*, et al.* (2015) Sustained Systemic Glucocerebrosidase Inhibition Induces Brain alpha-Synuclein Aggregation, Microglia and Complement C1q Activation in Mice. *Antioxid Redox Signal* 23(6):550-564.

30. Kim MJ, Jeon S, Burbulla LF, & Krainc D (2018) Acid ceramidase inhibition ameliorates alpha-synuclein accumulation upon loss of GBA1 function. *Hum Mol Genet* 27(11):1972-1988.

31. Sardi SP*, et al.* (2017) Glucosylceramide synthase inhibition alleviates aberrations in synucleinopathy models. *Proc Natl Acad Sci U S A* 114(10):2699-2704.

32. Mistry PK*, et al.* (2014) Glucocerebrosidase 2 gene deletion rescues type 1 Gaucher disease. *Proc Natl Acad Sci U S A* 111(13):4934-4939.

33. Tohyama J*, et al.* (2000) Paradoxical influence of acid beta-galactosidase gene dosage on phenotype of the twitcher mouse (genetic galactosylceramidase deficiency). *Hum Mol Genet* 9(11):1699-1707.

34. Austin-Tse C*, et al.* (2013) Zebrafish Ciliopathy Screen Plus Human Mutational Analysis Identifies C21orf59 and CCDC65 Defects as Causing Primary Ciliary Dyskinesia. *Am J Hum Genet* 93(4):672-686.

35. Ding Y*, et al.* (2016) A modifier screen identifies DNAJB6 as a cardiomyopathy susceptibility gene. *JCI Insight* 1(14).

36. Hosseinibarkooie S*, et al.* (2016) The Power of Human Protective Modifiers: PLS3 and CORO1C Unravel Impaired Endocytosis in Spinal Muscular Atrophy and Rescue SMA Phenotype. *Am J Hum Genet* 99(3):647-665.

37. Watson L*, et al.* (2019) Ablation of the pro-inflammatory master regulator miR-155 does not mitigate neuroinflammation or neurodegeneration in a vertebrate model of Gaucher's disease. *Neurobiol Dis*.

38. Hruscha A*, et al.* (2013) Efficient CRISPR/Cas9 genome editing with low off-target effects in zebrafish. *Development* 140(24):4982-4987.

39. Wilkinson RN, Elworthy S, Ingham PW, & van Eeden FJ (2013) A method for high-throughput PCR-based genotyping of larval zebrafish tail biopsies. *Biotechniques* 55(6):314-316.

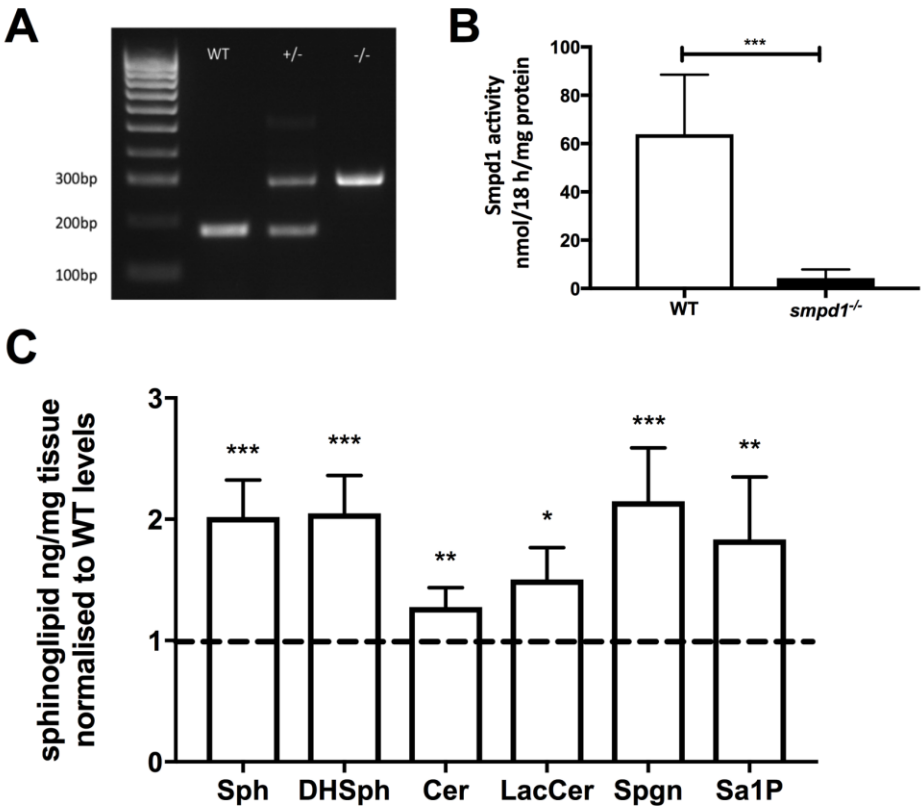

Fig. 1: (*A*) Representative genotyping gel of the *smpd1*$^{-/-}$ allele (5bp del and 136bp insertion) demonstrating WT, *smpd1*$^{+/-}$ and *smpd1*$^{-/-}$. (*B*) Acid sphingomyelinase (ASM) enzymatic activity was reduced by 93% in *smpd1*$^{-/-}$ 5dpf larvae (4.3 ± 1.447 nmol/18h/mg protein, n=6) compared to WT controls (63.86 ± 9.32 nmol/18h/mg protein, n=7), p=0.006 , Welch's t-test. (*C*) To determine the consequences of the loss of ASM enzymatic function, a panel of sphingolipid metabolites were analysed by mass spectrometry at 5dpf in WT and *smpd1*$^{-/-}$ larvae (n=5 per group each). These data were normalised to WT levels, indicated by the dashed line at 1.0. Sphingomyelin was elevated by 102%±30% above WT levels (Sph, p=0.0002). Dihydro-sphingomyelin was elevated by 105%±31% above WT levels (DHSph, p=0.0004). Ceramide was elevated by 27%±15% above WT levels (Cer, p=0.0067). Lactosylceramide was elevated by 51%±26% above WT levels (LacCer, p=0.0191). Sphinganine was elevated by 100%±43% above WT levels (Spgn, p=0.0007). Sphinganine 1 phosphate was elevated by 83%±51% above WT levels (Sa1P, p=0.093). All metabolites shown

are the C18 neuronal species. Data represented are the mean ±SD. Statistical analysis was performed using two-tailed t-test. ****p<0.0001, ***p<0.001, **p<0.01 and *p<0.05.

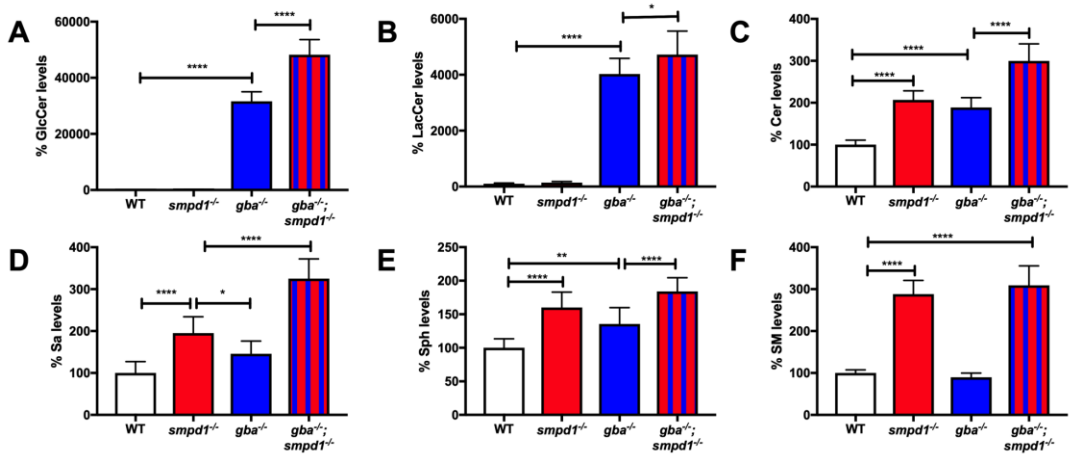

Fig. 2. Accumulation of key glycolipids across *gba1*$^{-/-}$; *smpd1*$^{-/-}$ and *gba1*$^{-/-}$; *smpd1*$^{-/-}$ genotypes. *(A)* Glucosylceramide levels (GlcCer) were quantified in *gba1*$^{-/-}$, *smpd1*$^{-/-}$ *and combined gba1*$^{-/-}$*; smpd1*$^{-/-}$ genotypes. GlcCer levels were dramatically increased by 31000%±3420% in *gba1*$^{-/-}$ compared to WT. GlcCer levels were increased further in *gba1*$^{-/-}$*; smpd1*$^{-/-}$ by 17000% compared to *gba1*$^{-/-}$ ($p<0.0001$) to 48000%±5376% compared to WT levels, ($p<0.0001$), demonstrating a synergy between both mutations on glucosylceramide levels. *(B)* Lactosylceramide levels were increased in *gba1*$^{-/-}$ and in double mutants by 4028%±558% and 4724%±836% respectively compared to WT levels ($p<0.0001$, for both), the increase of 696% ($p= 0.0191$) in *gba1*$^{-/-}$*; smpd1*$^{-/-}$ compared to *gba1*$^{-/-}$ demonstrated a synergy between both mutations on lactosylceramide levels ($p= 0.0191$). *(C)* Ceramide levels (Cer) were increased to a similar extent in in *smpd1*$^{-/-}$ (106%±21%) and *gba1*$^{-/-}$ (88%±23%) ($P<0.0001$ for both). This led to an additive effect in the *gba1*$^{-/-}$*; smpd1*$^{-/-}$ double mutants, which had significant increases in ceramide levels compared to all genotypes ($p<0.0001$ for all) the largest being a 199%±40% increase compared to WT. *(D)* Sphinganine (Sa) levels were increased in both *smpd1*$^{-/-}$ (95%±38% ($p<0.0001$) and *gba1*$^{-/-}$ 46%±30% ($p=0.0383$) compared to WT. *gba1*$^{-/-}$*; smpd1*$^{-/-}$ double mutants had a Sa accumulation of 325%±46% above WT levels that was significant against all genotypes ($p<0.0001$ for all). *(E)* Sphingosine (sph) levels across *gba1/smpd1*

genotypes were increased in *gba1*$^{-/-}$ and *smpd1*$^{-/-}$ of 35%±24% (p=0.0025) and 60%±23%(p<0.0001) respectively, with sph levels increased by 85%±20% above WT levels (p<0.0001) in *gba1*$^{-/-}$*; smpd1*$^{-/-}$*. (F)* Sphingomyelin (SM) levels were only increased in *smpd1*$^{-/-}$ (188%±32%) and *gba1*$^{-/-}$*; smpd1*$^{-/-}$ (209%±46%) respectively above WT levels (p<0.0001 for both). For all mass spec substrate analysis, N=10 of 12 week old brains used per group. Data represented are the mean ±SD. Statistical analysis was performed using 2 way Anova test with Tukeys multiple comparison. ****p<0.0001, ***p<0.001, **p<0.01 and *p<0.05.

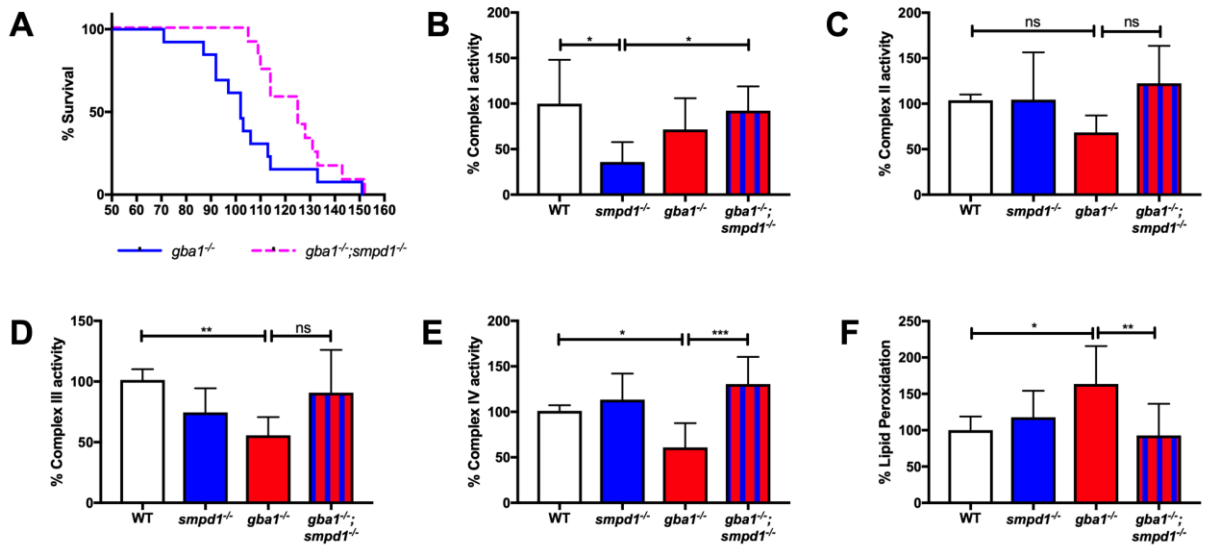

Fig. 3. Inhibition of acid sphingomyelinase activity results in improved survival of *gba*$^{-/-}$ zebrafish due to rescue of mitochondrial respiratory chain function in *gba1*$^{-/-}$;*smpd1*$^{-/-}$. *(A) gba1*$^{-/-}$;*smpd1*$^{-/-}$ have an increase in median survival time by 22% (125 days, n=13) compared to *gba1*$^{-/-}$ (102 days, n=12, p= 0.0055 Gehan-Breslow-Wilcoxon test). *(B)* Complex I activity is reduced in *smpd1*$^{-/-}$ by 64±34.77% compared to WT (p=0.0198). Complex I activity was normalized in *gba1*$^{-/-}$;*smpd1*$^{-/-}$ with an increase by 56±21.9% compared to *smpd1*$^{-/-}$ (p=0.0445). *(C)* Complex II activity was similar across the different genotypes. *(D)* Complex III activity was reduced in *gba1*$^{-/-}$ compared to WT by 45%±14.99 (p=0.0091), but increased by 35±35.2% in *gba1*$^{-/-}$;*smpd1*$^{-/-}$ compared to *gba1*$^{-/-}$ but this did not reach significance (p>0.05). *(E)* Complex IV activity was reduced in *gba1*$^{-/-}$ by 40%±26.79 compared to WT (p=0.0491), but completely rescued in *gba1*$^{-/-}$;*smpd1*$^{-/-}$ double mutants with an increase by 69±26.79% compared to *gba1*$^{-/-}$ (p=0.0005). *(F)* Lipid peroxidation levels were increased 63±51% in *gba1*$^{-/-}$ compared to WT (p=0.0214), but reduced by 71±43.48% compared to *gba1*$^{-/-}$ and thus effectively normalised to WT levels in *gba1*$^{-/-}$;*smpd1*$^{-/-}$ double mutants (p=0.0094). For all mitochondrial complex activity measurements, 6 brains were used for each genotype. For lipid peroxidation experiments, n= 6-8 zebrafish bodies were used for each genotype. Significance in both mitochondrial respiratory chain assays and lipid peroxidation levels was determined by two way ANOVA with Tukey's multiple

comparison test using 12 week brain material. Data represented are the mean ±SD. ***p<0.001, **p<0.01 and *p<0.05.

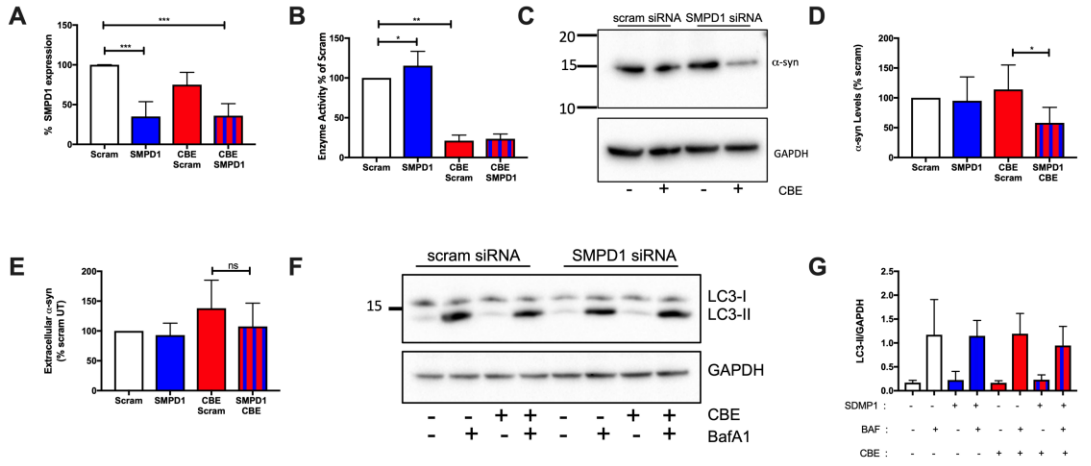

Fig. 4. The endolysosomal pathway is affected in human neuroblastoma cells following knockdown of *SMPD1*. *(A) SMPD1* transcript levels after *SMPD1* KD demonstrate a reduction of 65±19% and 64±15%, in untreated and CBE treated cells respectively; p =0.0003 (n=4) and 0.0007 (n=3), compared to controls. *(B)* GCase enzyme activity was increased by 15% in *SMPD1* KD compared to Scram control; p<0.0431 (n=7) and reduced by 77-79% in CBE treated groups compared to Scram untreated control; both p<0.0010 (n=7). *(C+D)* Western blotting for TX-100 soluble α-synuclein levels in *SMPD1* KD cells in the absence or presence of CBE. The levels of α-synuclein were decreased in *SMPD1 KD* + CBE cells by 56±26% p=0.0139; n=6) compared to scram CBE treated cells; p=0.0139 (n=6), when compared to CBE-treated cells. The latter had a 14% increase in levels compared to Scram untreated cells which did not reach significance. Data were normalised against GAPDH density and expressed as % scram. n = 6 for all groups. *(E)* α-synuclein levels released in to cell culture media from *SMPD1* KD cells in the absence and presence of CBE for the last 24 hours of treatment were assessed by ELISA. Data were normalised against protein concentration of cells and expressed as % Scram; No group showed significant changes to Scram untreated control group (n = 5). *(F+G)* Macroautophagy flux was measured by quantifying LC3-II protein levels using western blotting under basal conditions and following treatment with 100 nM bafilomycin A1 (BafA1) for 4 hours in *SMPD1* KD cells in the absence and presence of CBE. LC3-II protein levels were

normalised against GAPDH density and expressed as a ratio, n=3 for all groups. Two way ANOVA with Tukey's multiple comparison test. Data represented are the mean ±SD, ***p<0.001 and *p<0.05.

Video legends:

All videos were taken when the respective zebrafish were 12 weeks of age.

V-S1: Normal swimming behaviour in WT. All adults placed into a novel tank swim to the bottom momentarily before resuming standard swimming, balance and buoyancy maintained.

V-S2: Normal swimming behaviour in *smpd*$^{-/-}$. All adults placed into a novel tank swim to the bottom momentarily before resuming standard swimming, balance and buoyancy maintained.

V-S3: Markedly abnormal swimming behaviour in *gba*$^{-/-}$ with typical "corkscrew" swimming pattern. All adults placed into a novel tank swim in circular motions with balance and buoyancy defects. These increase with frequency and duration at end stage until they need to be culled for humane reasons.

V-S4: Normalised swimming behaviour in *gba*$^{-/-}$;*smpd*$^{-/-}$. All adults placed into a novel tank swim to the bottom momentarily before resuming standard swimming, balance and buoyancy maintained.

References:

1. Gasser T (2015) Usefulness of Genetic Testing in PD and PD Trials: A Balanced Review. *J Parkinsons Dis* 5(2):209-215.
2. Chang D*, et al.* (2017) A meta-analysis of genome-wide association studies identifies 17 new Parkinson's disease risk loci. *Nat Genet* 49(10):1511-1516.
3. Grabowski GA (2012) Gaucher disease and other storage disorders. *Hematology Am Soc Hematol Educ Program* 2012:13-18.
4. Platt FM (2014) Sphingolipid lysosomal storage disorders. *Nature* 510(7503):68-75.
5. Baris HN, Cohen IJ, & Mistry PK (2014) Gaucher disease: the metabolic defect, pathophysiology, phenotypes and natural history. *Pediatr Endocrinol Rev* 12 Suppl 1:72-81.
6. Neumann J*, et al.* (2009) Glucocerebrosidase mutations in clinical and pathologically proven Parkinson's disease. *Brain* 132(Pt 7):1783-1794.
7. Sidransky E*, et al.* (2009) Multicenter analysis of glucocerebrosidase mutations in Parkinson's disease. *N Engl J Med* 361(17):1651-1661.
8. Siebert M, Sidransky E, & Westbroek W (2014) Glucocerebrosidase is shaking up the synucleinopathies. *Brain* 137(Pt 5):1304-1322.
9. Anheim M*, et al.* (2012) Penetrance of Parkinson disease in glucocerebrosidase gene mutation carriers. *Neurology* 78(6):417-420.
10. O'Regan G, deSouza RM, Balestrino R, & Schapira AH (2017) Glucocerebrosidase Mutations in Parkinson Disease. *J Parkinsons Dis* 7(3):411-422.
11. Gan-Or Z*, et al.* (2015) Differential effects of severe vs mild GBA mutations on Parkinson disease. *Neurology* 84(9):880-887.
12. Robak LA*, et al.* (2017) Excessive burden of lysosomal storage disorder gene variants in Parkinson's disease. *Brain* 140(12):3191-3203.

13. Alcalay RN, *et al.* (2019) SMPD1 mutations, activity, and alpha-synuclein accumulation in Parkinson's disease. *Mov Disord* 34(4):526-535.

14. Simone BW, Martinez-Galvez G, WareJoncas Z, & Ekker SC (2018) Fishing for understanding: Unlocking the zebrafish gene editor's toolbox. *Methods* 150:3-10.

15. Keatinge M, *et al.* (2015) Glucocerebrosidase 1 deficient Danio rerio mirror key pathological aspects of human Gaucher disease and provide evidence of early microglial activation preceding alpha-synuclein-independent neuronal cell death. *Hum Mol Genet* 24(23):6640-6652.

16. Gegg ME & Schapira AH (2016) Mitochondrial dysfunction associated with glucocerebrosidase deficiency. *Neurobiol Dis* 90:43-50.

17. McKenna MC, Schuck PF, & Ferreira GC (2019) Fundamentals of CNS energy metabolism and alterations in lysosomal storage diseases. *J Neurochem* 148(5):590-599.

18. Mazzulli JR, *et al.* (2011) Gaucher disease glucocerebrosidase and alpha-synuclein form a bidirectional pathogenic loop in synucleinopathies. *Cell* 146(1):37-52.

19. Magalhaes J, *et al.* (2016) Autophagic lysosome reformation dysfunction in glucocerebrosidase deficient cells: relevance to Parkinson disease. *Hum Mol Genet* 25(16):3432-3445.

20. Perrotta C, *et al.* (2015) The emerging role of acid sphingomyelinase in autophagy. *Apoptosis* 20(5):635-644.

21. Li H, *et al.* (2019) Mitochondrial dysfunction and mitophagy defect triggered by heterozygous GBA mutations. *Autophagy* 15(1):113-130.

22. Osellame LD, *et al.* (2013) Mitochondria and quality control defects in a mouse model of Gaucher disease--links to Parkinson's disease. *Cell Metab* 17(6):941-953.

23. Campbell P, Morris H, & Schapira A (2018) Chaperone-mediated autophagy as a therapeutic target for Parkinson disease. *Expert Opin Ther Targets* 22(10):823-832.

24. Ysselstein D, Shulman JM, & Krainc D (2019) Emerging links between pediatric lysosomal storage diseases and adult parkinsonism. *Mov Disord*.

25. Lin G, Wang L, Marcogliese PC, & Bellen HJ (2019) Sphingolipids in the Pathogenesis of Parkinson's Disease and Parkinsonism. *Trends Endocrinol Metab* 30(2):106-117.

26. Cervia D*, et al.* (2016) Essential role for acid sphingomyelinase-inhibited autophagy in melanoma response to cisplatin. *Oncotarget* 7(18):24995-25009.

27. Justice MJ*, et al.* (2018) Inhibition of acid sphingomyelinase disrupts LYNUS signaling and triggers autophagy. *J Lipid Res* 59(4):596-606.

28. Lee JK*, et al.* (2014) Acid sphingomyelinase modulates the autophagic process by controlling lysosomal biogenesis in Alzheimer's disease. *J Exp Med* 211(8):1551-1570.

29. Rocha EM*, et al.* (2015) Sustained Systemic Glucocerebrosidase Inhibition Induces Brain alpha-Synuclein Aggregation, Microglia and Complement C1q Activation in Mice. *Antioxid Redox Signal* 23(6):550-564.

30. Kim MJ, Jeon S, Burbulla LF, & Krainc D (2018) Acid ceramidase inhibition ameliorates alpha-synuclein accumulation upon loss of GBA1 function. *Hum Mol Genet* 27(11):1972-1988.

31. Sardi SP*, et al.* (2017) Glucosylceramide synthase inhibition alleviates aberrations in synucleinopathy models. *Proc Natl Acad Sci U S A* 114(10):2699-2704.

32. Mistry PK*, et al.* (2014) Glucocerebrosidase 2 gene deletion rescues type 1 Gaucher disease. *Proc Natl Acad Sci U S A* 111(13):4934-4939.

33. Tohyama J*, et al.* (2000) Paradoxical influence of acid beta-galactosidase gene dosage on phenotype of the twitcher mouse (genetic galactosylceramidase deficiency). *Hum Mol Genet* 9(11):1699-1707.

34. Austin-Tse C*, et al.* (2013) Zebrafish Ciliopathy Screen Plus Human Mutational Analysis Identifies C21orf59 and CCDC65 Defects as Causing Primary Ciliary Dyskinesia. *Am J Hum Genet* 93(4):672-686.

35. Ding Y*, et al.* (2016) A modifier screen identifies DNAJB6 as a cardiomyopathy susceptibility gene. *JCI Insight* 1(14).

36. Hosseinibarkooie S*, et al.* (2016) The Power of Human Protective Modifiers: PLS3 and CORO1C Unravel Impaired Endocytosis in Spinal Muscular Atrophy and Rescue SMA Phenotype. *Am J Hum Genet* 99(3):647-665.

37. Watson L*, et al.* (2019) Ablation of the pro-inflammatory master regulator miR-155 does not mitigate neuroinflammation or neurodegeneration in a vertebrate model of Gaucher's disease. *Neurobiol Dis*.

38. Hruscha A*, et al.* (2013) Efficient CRISPR/Cas9 genome editing with low off-target effects in zebrafish. *Development* 140(24):4982-4987.

39. Wilkinson RN, Elworthy S, Ingham PW, & van Eeden FJ (2013) A method for high-throughput PCR-based genotyping of larval zebrafish tail biopsies. *Biotechniques* 55(6):314-316.